Promoter DNA methylation patterns in oral, laryngeal and oropharyngeal anatomical regions are associated with tumor differentiation, nodal involvement and survival

BIANCA RIVERA-PEÑA[1-3], OLUWASINA FOLAWIYO[4], NITESH TURAGA[4], ROSA J. RODRÍGUEZ-BENÍTEZ[5], MARCOS E. FELICI[6], JAIME A. APONTE-ORTIZ[7], FRANCESCA PIRINI[8], SEBASTIÁN RODRÍGUEZ-TORRES[9], ROGER VÁZQUEZ[1], RICARDO LÓPEZ[1], DAVID SIDRANSKY[4], RAFAEL GUERRERO-PRESTON[4,10] and ADRIANA BÁEZ[2,3]

[1]Department of Biology, University of Puerto Rico, San Juan 00925; Departments of [2]Pharmacology and [3]Otolaryngology-Head and Neck Surgery, University of Puerto Rico School of Medicine, San Juan 00936, Puerto Rico; [4]Department of Otolaryngology-Head and Neck Surgery, Johns Hopkins University School of Medicine, Baltimore, MD 21231, USA; [5]Department of General Social Sciences, Faculty of Social Sciences, University of Puerto Rico, San Juan 00925; [6]Oral Health Division, Puerto Rico Department of Health, San Juan 00927; [7]Department of General Surgery, University of Puerto Rico School of Medicine, San Juan 00936, Puerto Rico; [8]Biosciences Laboratory, IRCCS Instituto Romagnolo per lo Studio dei Tumori 'Dino Amadori', Meldola I-47014, Italy; [9]Department of Medicine, University of Pittsburgh School of Medicine, Pittsburgh, PA 15213, USA; [10]Department of Research and Development, LifeGene-Biomarks, San Juan 00909, Puerto Rico

Received April 8, 2023; Accepted November 23, 2023

DOI: 10.3892/ol.2024.14223

Abstract. Differentially methylated regions (DMRs) can be used as head and neck squamous cell carcinoma (HNSCC) diagnostic, prognostic and therapeutic targets in precision medicine workflows. DNA from 21 HNSCC and 10 healthy oral tissue samples was hybridized to a genome-wide tiling array to identify DMRs in a discovery cohort. Downstream analyses identified differences in promoter DNA methylation patterns in oral, laryngeal and oropharyngeal anatomical regions associated with tumor differentiation, nodal involvement and survival. Genome-wide DMR analysis showed 2,565 DMRs common to the three subsites. A total of 738 DMRs were unique to laryngeal cancer (n=7), 889 DMRs were unique to oral cavity cancer (n=10) and 363 DMRs were unique to pharyngeal cancer (n=6). Based on the genome-wide analysis and a Gene Ontology analysis, 10 candidate genes were selected to test for prognostic value and association with clinicopathological features. *TIMP3* was associated with tumor differentiation in oral cavity cancer (P=0.039), *DAPK1* was associated with nodal involvement in pharyngeal cancer (P=0.017) and *PAX1* was associated with tumor differentiation in laryngeal cancer (P=0.040). A total of five candidate genes were selected, *DAPK1, CDH1, PAX1, CALCA* and *TIMP3*, for a prevalence study in a larger validation cohort: Oral cavity cancer samples (n=42), pharyngeal cancer tissues (n=25) and laryngeal cancer samples (n=52). *PAX1* hypermethylation differed across HNSCC anatomic subsites (P=0.029), and was predominantly detected in laryngeal cancer. Kaplan-Meier survival analysis (P=0.043) and Cox regression analysis of overall survival (P=0.001) showed that *DAPK1* methylation is associated with better prognosis in HNSCC. The findings of the present study showed that the HNSCC subsites oral cavity, pharynx and larynx display substantial differences in aberrant DNA methylation patterns, which may serve as prognostic biomarkers and therapeutic targets.

Correspondence to: Dr Adriana Báez, Department of Otolaryngology-Head and Neck Surgery, University of Puerto Rico School of Medicine, 960 Américo Miranda Avenue, San Juan 00936, Puerto Rico
E-mail: adriana.baez@upr.edu

Dr Rafael Guerrero-Preston, Department of Research and Development, LifeGene-Biomarks, San Juan 00909, Puerto Rico
E-mail: rguerrero@lifegenedna.com

Abbreviations: HNSCC, head and neck squamous cell carcinoma; HPV16, human papillomavirus 16; LSCC, larynx squamous cell carcinoma; OSCC, oral cavity squamous cell carcinoma; OPSCC, oropharynx squamous cell carcinoma; DMRs, differentially methylated regions; OS, overall survival; qPCR, quantitative polymerase chain reaction; TSGs, tumor suppressor genes; MeDIP, methylated DNA immunoprecipitation; TSS, transcription starting site; TCGA, The Cancer Genome Atlas; GO, Gene Ontology; IP DNA, immunoprecipitated DNA; WGA, whole genome amplification

Key words: differentially methylated regions, precision medicine, head and neck squamous cell carcinoma survival, prognostic biomarkers, epigenome-wide analysis

Introduction

Head and neck squamous cell carcinoma (HNSCC) is the 6th most common malignancy and the 8th cause of cancer

death worldwide (1,2). HNSCC includes carcinomas from the oral cavity (OSCC), oropharynx (OPSCC), hypopharynx (HPSCC), larynx (LSCC), the paranasal sinuses, and the major and minor salivary glands. The etiology of HNSCC involves a variety of toxic, environmental and viral agents (3). Tobacco and alcohol exposure are the primary etiological factors for HNSCC (4-6). Oncogenic human papillomavirus (HPV) strains, primarily HPV-16, have been recognized as risk factor for HNSCC, particularly for oropharyngeal cancers (7-10). Men are more frequently diagnosed with HNSCC compared with women, and the incidence of HNSCC has a male-to-female ratio of 3:1 in the US (11). This incidence has been changing as women increasingly expose themselves to HNSCC risk factors, tobacco, alcohol and HPV-infection. Park *et al* (12) showed that women with HNSCC are at a higher risk of dying of the disease than men diagnosed with HNSCC (HR=1.92; 95% CI, 1.07-3.43). However, HPV-associated HNSCC is more common in men compared with women (13). Patients with HPV^+ HNSCC have a better prognosis than patients with HPV^- HNSCC (14); HPV may have a role in the clinical manifestation of this sex disparity. HNSCC is commonly diagnosed in patients ≥60 years old, however, an increasing number of patients are diagnosed with HNSCC at younger ages (15). Most patients with HNSCC are diagnosed at advanced stages of the disease (III or IV), which leads to a poor prognosis outcome (16). HNSCC treatment is generally multimodal including surgery, rand chemoradiation, yet the overall survival (OS) of patients with HNSCC is relatively low, ~2.5 years after treatment, for all HNSCC sites and stages (17).

In the US, African Americans, Hispanics/Latinos and low-income non-Latino-White individuals are at higher risk of developing HNSCC. In Puerto Rico, the incidence of HNSCC is 2.5 times higher than that in Hispanics/Latinos living in the US. The HNSCC incidence of OSCC and OPSCC is 72% higher in Puerto Rico than among Hispanics/Latinos living in the US. Similarly, the incidence of LSCC in Puerto Rico is 51% higher than that in Hispanics/Latinos living in the US (18). Racial and ethnic health disparities are a serious public health concern due to the HNSCC high mortality and morbidity rates, higher treatment costs and the effect on quality of life. Therefore, discovery of actionable targets for the early detection, diagnosis and prognosis of HNSCC, and for guiding treatment would have an immediate impact on reducing these health disparities.

Epigenetic biomarkers, such as aberrant DNA methylation changes, have been used as molecular classifiers for different cancer types, having a predictive capacity for patient prognosis and treatment response (19). Aberrant changes in DNA methylation such as global DNA hypomethylation and specific promoter DNA hypermethylation have been associated with carcinogenesis (20). It has been proposed that aberrant changes in DNA methylation patterns occur early in the carcinogenic process (21).

Aberrant promoter methylation of tumor suppressor genes (TSGs), for instance, *CDH1*, *DAPK1*, *CDKN2A* and *RASSF1A*, have been detected in HNSCC that resulted in loss of expression and pathway deregulation (22-24). Several studies have demonstrated DNA methylation cancer-related signatures (25,26), suggesting the likelihood of differential DNA methylation patterns among HNSCC anatomical subsites (27). Using a candidate gene approach, the prevalence of the aberrantly methylated TSGs *CDKN2A*, $p14^{ARF}$ *and CDKN2B* in HNSCC tumors was previously evaluated. Bernabe (28) detected aberrant methylation of the TSGs *CDKN2A* and *CDKN2B* in HNSCC tumors. A reduction of *CDKN2A* expression in HNSCC tumors exhibiting methylated (M) *CDKN2A* was detected with mRNA expression analysis (28). Subsequently, the aberrant methylation of *CDH1* was evaluated in HNSCC tumors confirming its occurrence, but hyperM *CDH1* was predominantly detected in the larynx compared with other HNSCC subsites (29). Preliminary data suggest that a distinct pattern of aberrant DNA methylation changes may occur in HNSCC anatomic subsites associated with HNSCC heterogeneity and its diverse clinical manifestations.

The primary objective of the present study was to perform a genome-wide DNA methylation analysis in HNSCC samples from three anatomic subsites, oral cavity, oropharynx and larynx, to identify potential DNA methylation targets with prognostic value for HNSCC. Furthermore, a prevalence assessment of selected candidate genes was performed, and their prognostic value was evaluated in an independent HNSCC cohort. It was hypothesized that a biomarker profile based on aberrant DNA methylation specific to every anatomical site, may help clinicians to better diagnose HNSCC, thus providing a more accurate prognosis and identify targets for novel treatments.

Materials and methods

HNSCC discovery cohort. Demographics and clinicopathological characteristics of the HNSCC discovery and prevalence cohorts are shown in Table I. The HNSCC discovery cohort included 21 HNSCC tissue samples from Puerto Rican patients, including 10 OSCC, four OPSCC and seven LSCC samples. The HNSCC discovery cohort samples were compared with 10 healthy oral tissue samples. The mean age of the discovery cohort was 56.62 years (range, 24-76 years; SD, 12.62), and 90 and 10% of patients were male and female, respectively. The HNSCC anatomical subsite distribution included 48, 19 and 33% oral cavity, pharynx and larynx, respectively. Most of the patients with HNSCC were at advanced stages (III/IV; 67%) of the disease. A total of 1/3 of the patients (33%) were HPV^+. Most tumors showed moderate differentiation (71%). Most samples were obtained from heavy smokers (95%) and heavy drinkers (86%).

HNSCC prevalence cohort. The HNSCC prevalence cohort included 119 HNSCC tissue samples from three anatomical subsites: Oral cavity (n=42), pharynx (n=25) and larynx (n=52). The HNSCC tissue samples of the prevalence cohort were compared with seven healthy oral tissue samples. The mean age of the HNSCC prevalence cohort was 61.2 years (range, 24-98 years; SD, 12.6), and 89.9 and 10.1% were male and female, respectively. The distribution of the HNSCC anatomical subsites included 35.3, 21.0 and 43.7% oral cavity, pharynx and larynx, respectively. Most of the patients with HNSCC were at advanced stages (III/IV; 77%) of the disease. Regarding HPV infection, 47.9% of patients were HPV^+. Most tumors showed moderate differentiation (65.5%). Most samples were obtained from heavy smokers (87%) and heavy drinkers (84%).

Table I. Clinicopathological characteristics of the head and heck squamous cell carcinoma discovery cohort (n=21) and the prevalence cohort (n=119).

Characteristics	Discovery cohort	Prevalence cohort
Age, years	56.62±12.62 (24-76)	61.21±12.63 (24-98)
Sex, n (%)		
Male	19 (90.5)	107 (89.9)
Female	2 (9.5)	12 (10.1)
Site of primary tumor, n (%)		
Oral cavity	10 (47.6)	42 (35.3)
Pharynx	4 (19.1)	25 (21.0)
Larynx	7 (33.3)	52 (43.7)
Tumor stage, n (%)[a]		
Early (I/II)	7 (33.3)	25 (21.0)
Advanced (III/IV)	14 (66.7)	92 (77.3)
HPV-16 status, n (%)[a]		
HPV-16$^+$	7 (33.3)	57 (47.9)
HPV-16$^-$	12 (57.1)	62 (52.1)
Differentiation, n (%)[b]		
Poor	2 (9.5)	9 (7.6)
Moderate	15 (71.4)	78 (65.5)
Well	4 (19.1)	31 (26.1)
Heavy smoking, n (%)	20 (95.2)	104 (87.4)
Heavy drinking, n (%)	21 (100.0)	97 (81.5)

[a]Data was not available for 2 patients. [b]Data was not available for 1 patient. Data are shown as mean ± SD (range). HPV, human papillomavirus.

The HNSCC tissue samples for both discovery and prevalence cohorts were obtained from Puerto Rican patients with HNSCC presenting at the School of Medicine Head and Neck Cancer Clinic at the Puerto Rico Medical Center, a tertiary teaching medical center. Patients that were diagnosed with HNSCC through tissue biopsy, and whose tumors were surgically removed signed an informed consent. The tumor tissue collected for the study was analyzed for quality by a pathologist. Oral mucosa samples were obtained from healthy Puerto Rican patients undergoing a routine tooth extraction at the School of Dental Medicine, Department of Surgery after having signed an informed consent. All procedures had the approval of the University of Puerto Rico, Medical Sciences Campus Institutional Review Board (IRB; approval no. MSC-IRB protocol 2770103), and the Johns Hopkins School of Medicine IRB (approval no. NA_00020633). The medical information of the patients with HNSCC was obtained from medical records and pathological reports, including date of diagnosis, site of the primary tumor, tumor grade, date and site of tumor recurrence (if applicable), and date and cause of death. The treatment of choice was surgery followed in some cases by postoperative radiation or chemoradiation. Follow-up information was prospectively collected from either medical records or the Puerto Rican Cancer Registry. Fig. 1 shows an integrated diagram describing the experimental study design.

DNA extraction. Genomic DNA was isolated from all HNSCC and healthy tissues using the DNA Isolation kit for cells and tissues (catalog no. 11814770001; Roche Diagnostics, Ltd.) following the manufacturer's instructions. DNA concentration and quality were measured with the NanoDrop 8000 UV-Vis Spectrophotometer (Thermo Fisher Scientific, Inc.). DNA sample preparation and hybridization to oligonucleotide arrays was carried out at the Head and Neck Cancer Research laboratory, Johns Hopkins School of Medicine.

Detection of HPV-16. Genomic DNA from all HNSCC samples was analyzed for HPV-16 infection. The HPV-16 status was previously detected by immunohistochemistry, end-point PCR and a TaqMan-based quantitative (q)PCR assay, targeting HPV-16 E6 and E7 viral oncogenes. All the HNSCC samples that were classified as HPV-16$^+$ had amplification of E6 and E7 viral oncogenes detected through a qPCR assay. HPV-16 E6 and E7 specific primer and probe sets, and qPCR and thermal cycling conditions were previously described (10).

Genome-wide DNA methylation analysis

DNA sonication. Two different genomic DNA amounts from HNSCC and healthy samples from the discovery cohort (0.5 and 1 μg) were used as input DNA for sonication to generate 200-800-bp long DNA fragments. DNA sonication was performed in a Covaris E220 ultrasonicator (Covaris, LLC), and analysis of sonicated DNA was performed on the BioAnalyzer 2100 (Agilent Technologies, Inc.) with an Agilent High Sensitivity DNA Kit (catalog no. 5067-4626; Agilent Technologies, Inc.) to verify DNA concentration, quality and purity.

Methylated DNA immunoprecipitation. DNA from HNSCC and healthy samples from the discovery cohort was subjected to methylated DNA immunoprecipitation (MeDIP) using the MagMeDIP kit (Diagenode SA) following the manufacturer's instructions. Two different starting DNA quantities were used (0.5 and 1 μg) for every sonicated sample. A total of 10% of every sample was transferred to a 1.5-ml tube (input DNA) and used as control of the starting DNA material. The remaining 90% of the sonicated DNA was subjected to MeDIP and labeled as immunoprecipitated DNA (IP DNA). IP DNA samples were exposed to a 5-methylcytosine antibody, which recognizes methylated cytosines in the DNA to enrich every sample with methylated DNA. Every tumor or control (healthy) DNA sample had an IP DNA and an input DNA. Samples were subjected to a qPCR assay to determine the efficiency of the MeDIP assay efficiency in enriching methylated DNA. IP DNA samples were compared with input DNA samples to determine if enrichment of methylated DNA occurred. Both DNA samples were tested using four primer pairs included in the MagMeDIP kit (Diagenode SA; Table SI).

The qPCR master mix included the following: 6.25 μl SYBR Green Supermix, 0.5 μl primer pair (10 μM), 3.5 ng either IP DNA or input DNA, and 3.25 μl water. The final reaction volume was 12.5 μl. The thermocycling conditions involved a denaturation step at 95˚C for 7 min, followed by

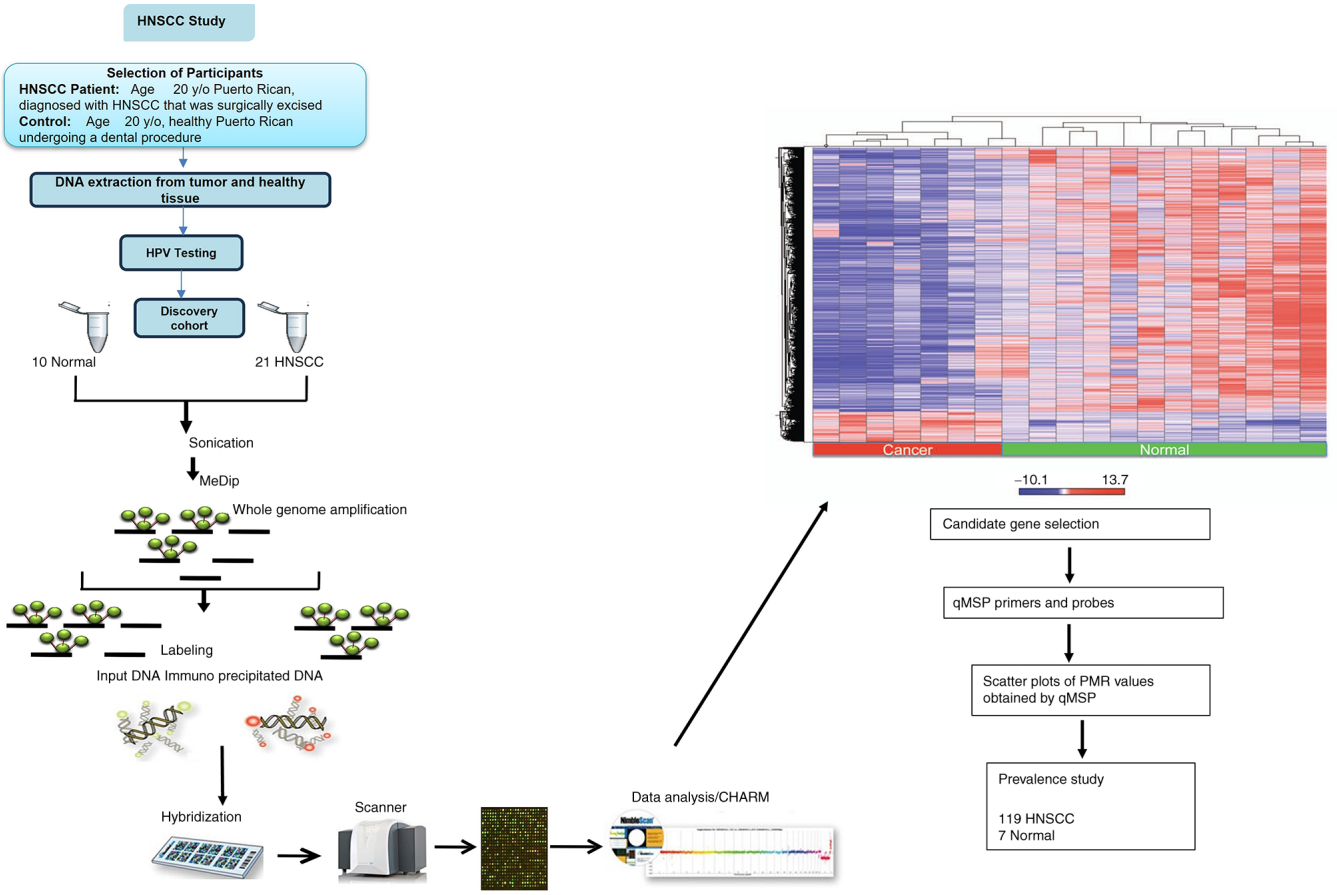

Figure 1. Flow chart showing the integrated experimental design of the present study. HNSCC, head and neck squamous cell carcinoma; HPV, human papillomavirus; MeDIP, methylated DNA immunoprecipitation; CHARM, comprehensive high-throughput arrays for relative methylation; qMSP, quantitative methylation-specific PCR; PMR, percentage of methylated reference.

40 cycles at 95˚C for 15 sec and at 60˚C for 1 min, an incubation step for 95˚C for 1 min to denature the DNA, and a melting curve analysis as established by the manufacturer instructions. The efficiency of MeDIP enrichment was calculated using the following equation: % (meDNA-IP/total input)=$2^{[(Cq(10\%input)-3.32)-Cq(meDNA-IP)]\ x100}$. The MeDIP recovery was % (meDNA-IP/total input). Samples that showed >50% DNA methylation enrichment were subjected to hybridization and scanning into the 3x720K CpG Island Plus RefSeq Promoter Array (Roche Diagnostics, Ltd.; Fig. S1).

DNA labeling and hybridization. After the MeDIP assay, all DNA samples (IP DNA and input DNA) were subjected to a genome-wide amplification (WGA) assay (Sigma-Aldrich; Merch KGaA) to increase the amount of DNA in every sample. After the WGA assay, DNA samples were purified using the QIAquick PCR Purification Kit (Qiagen Sciences, Inc.). DNA concentration was measured with the NanoDrop 8000 UV-Vis Spectrophotometer (Thermo Fisher Scientific, Inc.). Every DNA sample (IP DNA and input DNA) was labeled with fluorophores using the NimbleGen Dual-Color DNA Labeling Kits (Roche Diagnostics, Ltd.). IP DNA was labeled with Cy5 fluorophore, and the input DNA was labeled with the Cy3 fluorophore. Labeled IP DNA and input DNA samples were combined and hybridized into the 3x720K CpG Island Plus RefSeq Promoter Array. Hybridization was accomplished using the NimbleGen Hybridization Kit (Roche Diagnostics, Ltd.) following standard operating protocol. The 3x720K CpG Island Plus RefSeq Promoter Array allowed hybridization of three samples simultaneously and covered 27,728 annotated CpG islands, 22,532 RefSeq gene promoters, and regulatory elements from the HG18 build. Each promoter array included several positive, negative and non-CpG control regions to calculate experimental performance. Analysis of RefSeq gene promoters involved regions 2.4 kb upstream of the transcription start site (TSS) and 0.6 kb downstream of the TSS for overall coverage of 3 kb of each promoter per gene. Each array was scanned in the NimbleGen MS2 Microarray Scanner (Roche Diagnostics, Ltd.) following the manufacturer's protocol.

Differential methylation bioinformatics. NimbleGen's DeVa's software (Roche Diagnostics, Ltd.) was used to create .xys files from the array's scanned images. The images allowed a peak discovery algorithm to generate an initial list of differentially methylated regions (DMRs) when tumor samples were compared with control samples. The .xys files were used as input data for the analysis using Comprehensive high-throughput arrays for relative methylation (CHARM) bioinformatics package within the R 4.1.2 statistical programming (30). CHARM software is a bioinformatics package used to discover DMRs between samples, calculate the percentage of methylation, verify array quality and control

for batch effects. Besides, DMRs were identified with Bump Hunting (version 1.44.0) (31), a statistical genomics tool to identify differential peaks in methylation data. Methylation Bump Hunting is a data analysis pipeline that effectively models measurement error, removes batch effects, detects regions of interest, and attaches statistical uncertainty to regions identified as differentially methylated (32). The bioinformatical analysis pipeline used in the present study included analysis of TSS and CpG Islands independently among tumor and control samples (Data S1). Frequency of genes was analyzed for tumor and control samples. Genes with a frequency of ≥20% in tumor samples were selected. Likewise, commonly occurring genes between tumor and control samples were analyzed. A detailed bioinformatical pipeline description for peak discovery algorithm can be found in Data S1. In summary, the raw intensity data from the array were analyzed and the data was transformed into a log ratio of the intensities of methylated probes vs. unmethylated probes, which represents the M-value. An M-value ~0 represented a similar intensity between the methylated and unmethylated probes. Positive M-values implied that more molecules within the tested probe were methylated than negative M-values, which represented less methylation (32). An M-value cut-off was established to define which CpG targeted sites were aberrantly methylated in tumor samples compared with control samples. CpG targeted sites with an M-value ≥2.0 were classified as methylated and were further analyzed. CpG sites with an M-value <2.0 were classified as unmethylated. CpG targeted sites were also subjected to a low-stringency P-value threshold (P<0.05) and ranked by fold-change between tumor and control samples. A list of DMRs was created using the CpG sites methylation level for every HNSCC subsite. These lists determined the regions in the genome that were differentially methylated between HNSCC and normal samples.

DMR validation in TCGA. DMRs identified through bioinformatical analyses were cross-referenced with available methylation-related databases, including publicly available HNSCC TCGA methylation database and peer-reviewed accessible databases, as previously described (33). Briefly, the Bump Hunting method was used to perform an epigenome-wide analysis of the HNSCC methylome to identify DMRs of biological interest using methylation arrays. Two separate epigenome-wide analyses were carried out using Bioconductor's minfi package (version 1.48.0), as previously described (34). Briefly, an unbiased epigenome-wide DNA methylation analysis was performed using the minfi package in Bioconductor to identify DMRs in 274 primary chemotherapy-naïve HNSCC samples (TCGA dataset) and 32 frequency-matched uvulopalatopharyngoplasty (UPPP) controls (Johns Hopkins Head and Neck Cancer Research laboratory). The significant DMRs (P<0.001) were identified in a CpG island located ≤200 bp upstream and downstream from the 5' end of the gene. The DMRs results obtained with MeDIP were validated with DMRs results from HNSCC TCGA samples. Significant DMRs common to both sample sets were subjected to Gene Ontology (GO) analysis with Database for Annotation, Visualization and Integrated Discovery version 6.7 (https://david.ncifcrf.gov/tools.jsp).

Candidate gene selection. Based on the genome wide DMR analysis, TCGA comparison and GO bioinformatics analysis, the 10 genes *DAPK1, PITX2, PAX5, TIMP3, SFRP1, CALCA, SOCS1, CDH1, MAGI2* and *PAX1* were selected for downstream validation as candidate biomarker genes for HNSCC, using quantitative methylation-specific PCR (qMSP).

DNA bisulfite modification. Bisulfite modification was used to convert unmethylated cytosine residues of genomic DNA into uracil while leaving the methylated cytosines unchanged. For all HNSCC and healthy samples, including discovery and prevalence cohort, 1 μg genomic DNA was treated with sodium bisulfite using the EZ DNA Methylation-Gold Kit (catalog no. D5005; Zymo Research Corp.) according to the manufacturer's protocol.

qMSP. All HNSCC and healthy DNA samples, including the discovery and prevalence cohorts, were subjected to qMSP. Tumor and healthy bisulfite-modified DNA samples were used as a qMSP assay template, a fluorescence-based real-time PCR assay was previously described (35). Primers and probe set sequences selected had been previously described to amplify the promoter regions of *DAPK1, PITX2, PAX5, TIMP3, SFRP1, CALCA, SOCS1, CDH1, MAGI2* and *PAX1*, and a reference gene, *ACTβ*. Primers and probe set sequences are shown in Table SII (36-43). All qMSPs were carried out in duplicates in a 48-well reaction plate with a final volume of 25 μl. Each reaction contained 600 nM forward and reverse primers, 200 nM probe (Integrated DNA Technologies, Inc.), 1x TaqMan Universal PCR Master Mix, no UNG (Thermo Fisher Scientific, Inc.) and 2 μl bisulfite-modified DNA. qMSP amplifications were performed in a StepOne Real-Time PCR System (Thermo Fisher Scientific, Inc.) using the following conditions: 95˚C for 10 min, followed by 40 cycles of 95˚C for 15 sec and an annealing temperature of 58˚C for 1 min. Each reaction plate included HNSCC bisulfite-modified DNA samples, a positive, fully methylated DNA control sample (bisulfite-converted Universal Methylated Human DNA Standard; Zymo Research Corp.) and no-template controls. Serial dilutions (30-0.003 ng) of bisulfite-converted Universal Methylated Human DNA standard were used to construct a calibration curve for each plate. After amplification, the percentage of methylated reference (PMR) for each candidate gene in each sample was calculated using the following equation: [(HNSCC sample Cq value gene of interest/HNSCC sample Cq value β-actin)/(fully methylated sample Cq value gene of interest/fully methylated sample Cq value β-actin] x100.

PMR values obtained from samples from the discovery cohort were used to draw receiver operating characteristic (ROC) curves to obtain sensitivity and specificity values for every candidate gene. ROC curves were drawn using STATA (version 15; StataCorp LP). Based on sensitivity and specificity values, a suitable PMR cut-off value was chosen for every candidate gene. Prevalence cohort samples were classified as methylated (M) or unmethylated (UM) based on the PMR cut-off value for every candidate gene. Promoter methylation of *PITX2, PAX5* and *TIMP3* was tested in 29 OSCC samples. Promoter methylation of *SFRP1, CALCA* and *SOCS1* was tested in 19 OPSCC samples. Promoter methylation of *CDH1,*

Table II. Predictive accuracy of *DAPK1, PITX2, PAX5, TIMP3, SFRP1, CALCA, SOCS1, CDH1, MAGI2* and *PAX1* for head and neck squamous cell carcinoma.

Target genes	ROC	P-value	Sensitivity, %	Specificity, %	Methylation cut-off value
DAPK1	0.92	0.0009	88.89	100.00	12.36
PITX2	1.00	<0.0001	100.00	100.00	16.37
PAX5	0.96	<0.0001	88.89	100.00	15.71
TIMP3	1.00	<0.0001	100.00	100.00	4.52
SFRP1	0.96	0.0005	100.00	90.00	12.47
CALCA	0.90	0.0006	85.71	100.00	26.37
SOCS1	0.52	0.4750	57.14	90.00	4.06
CDH1	0.82	0.0054	75.00	90.00	16.15
MAGI2	0.96	0.0001	87.50	100.00	20.86
PAX1	1.00	<0.0001	100.00	100.00	29.41

ROC, receiver operating characteristic curve.

MAGI2 and *PAX1* was tested in 39 LSCC samples. Promoter methylation of *DAPK1* was used as an internal control and was evaluated in all HNSCC samples.

Statistical analysis. Data from independent groups were compared using Fisher's exact test or χ^2-test, as appropriate. Odds ratio (OR) calculations for clinicopathological parameters were performed using binary logistic. OS was measured in months from the date of diagnosis until death (if applicable). Survival analyses were performed using Kaplan-Meier curves. Log-rank Mantel-Cox and Gehan-Breslow Wilcoxon tests were used to determine the significance between two survival curves. Prognostic factors that have impact on HNSCC survival were analyzed in a Cox regression analysis. Statistical analyses were performed using SPSS (version 22; IBM Corp.). P<0.05 was considered to indicate a statistically significant difference.

Results

DMRs in HNSCC tumor samples from the discovery cohort. Results from the discovery cohort show that the three HNSCC subsites had in common 2,565 DMRs that included genes previously associated with HNSCC (Table SIII). Some of the identified DMRs corresponded to genes previously described as having a pivotal role in HNSCC carcinogenesis, such as *BRCA2, CDKN2A, CDKN1B (P27), DAPK1,MAPK1, MAPK10, MLH1, RASSF1, HOXC6, VEGFB, WNT1* and *WNT8B* (44-55). Among these genes, several of them have roles in essential pathways for cell cycle regulation (*RASSF1* and *CDKN1B)*, cell proliferation *(MAPK1* and *MAPK10)* and apoptosis (*DAPK1*).

The genome-wide analysis also unveiled 889 DMRs unique for OSCC, 363 DMRs for OPSCC and 738 DMRs for LSCC (Fig. S2). Results from the 450K Infinium DNA methylation array from 274 HNSCC TCGA samples and 32 frequency-matched UPPP control samples from John Hopkins Head and Neck Cancer Research Laboratory were used to validate subsite-specific DMRs identified in the MeDIP experiment. A GO analysis was used to describe the function of the most critical DMRs. Based on the DMR and GO analyses, *DAPK1, PITX2, PAX5, TIMP3, SFRP1, CALCA, SOCS1, CDH1, MAGI2* and *PAX1* were selected as candidate genes to be further evaluated.

The promoter methylation status of the 10 candidate genes in all HNSCC and healthy samples from the discovery cohort was analyzed. Samples were subjected to qMSP analysis for all candidate genes. A total of nine candidate genes showed differential methylation between HNSCC and healthy samples. The candidate gene *SOCS1* showed no difference in the promoter methylation status between HNSCC and healthy samples. Table II shows values obtained for sensitivity, specificity, ROC curve and PMR cut-off value for every candidate gene.

In the OSCC samples, M *PITX2* and *PAX5* were detected in 58.6 and 79.3% of the samples, respectively. Also, M *TIMP3* was confirmed in 79.3% of the samples, and M *DAPK1* was detected in 51.7% of the samples. In the OPSCC samples, M *SFRP1, CALCA* and *SOCS1* were detected in 84.2, 78.9 and 15.8% of the samples, respectively. M *DAPK1* was detected in 63.2% of the samples. As for LSCC samples, M *CDH1, MAGI1* and *PAX1* were detected in 58.9, 64.1 and 74.4% of the samples, respectively. M *DAPK1* was detected in 66.7% of the LSCC samples.

A total of five candidate genes were selected, *DAPK1, CDH1, PAX1, CALCA* and *TIMP3*, for validation in a HNSCC prevalence cohort based on predictive accuracy of the genes. Each candidate gene's predictive accuracy to detect HNSCC was calculated by ROC curve analysis. The sensitivity and specificity values were used to select the PMR cut-off value for every candidate gene. *PAX1* and *TIMP3* had ROC values of 1.00, 100% sensitivity and 100% specificity; *DAPK1* had a ROC value of 0.92, 88.9% sensitivity and 100% specificity; *CALCA* had a ROC value of 0.90, 85.7% sensitivity and 100% specificity; and *CDH1* had a ROC value of 0.82, 75% sensitivity and 90% specificity.

A PMR value was calculated for every candidate gene for all HNSCC and healthy samples in the prevalence cohort. PMR values obtained from the prevalence cohort were

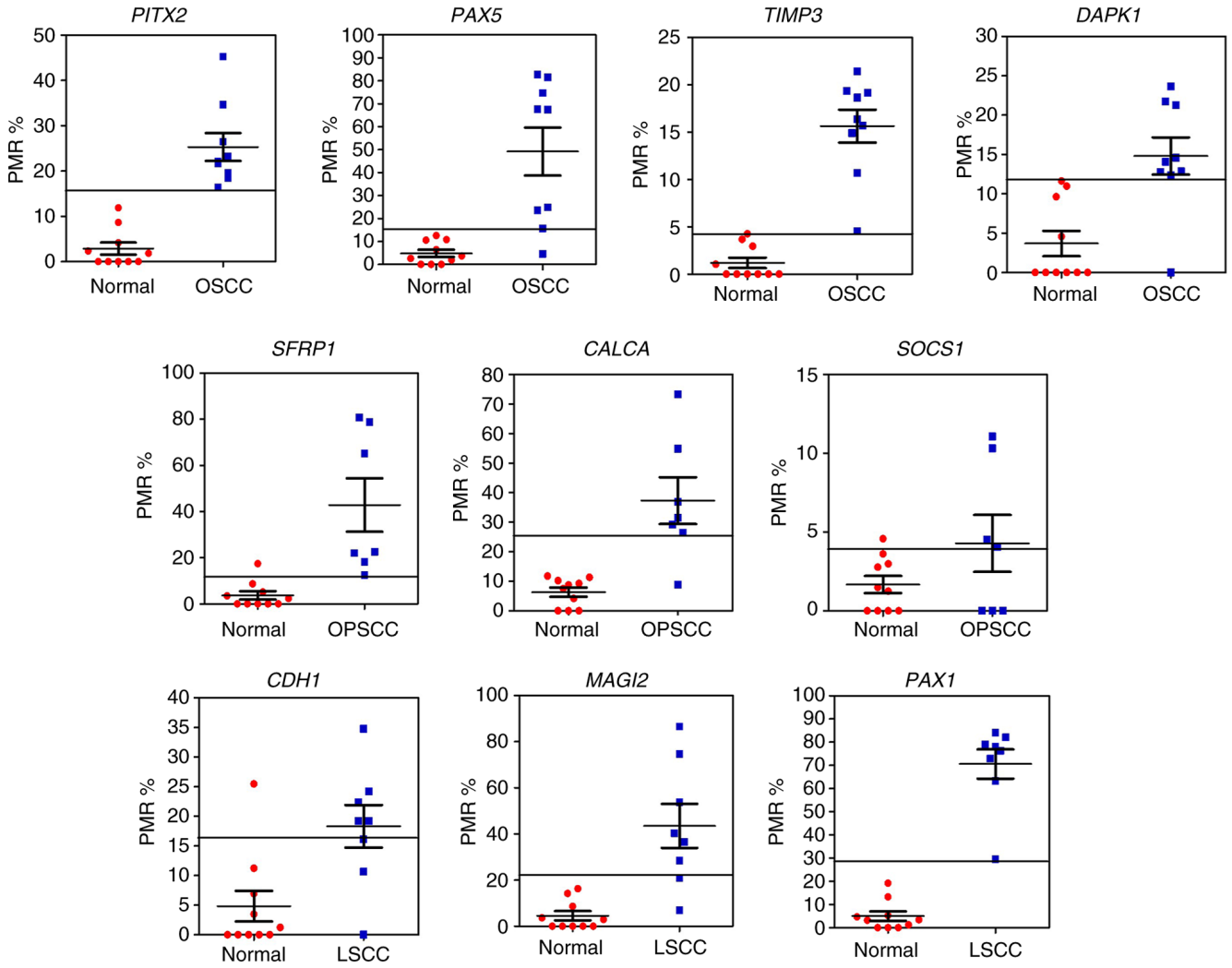

Figure 2. Scatterplots of the PMR values obtained by qMSP in the analysis of selected candidate genes in the discovery cohort. The PMR for every candidate gene was expressed as a ratio of the amplification from the target gene to the amount amplified from the reference gene β-actin, then multiplied by 100. The black line represents the PMR cut-off value for each candidate gene. PMR, percentage of methylated reference; qMSP, quantitative methylation-specific PCR; LSCC, larynx squamous cell carcinoma; OSCC, oral cavity squamous cell carcinoma; OPSCC, oropharynx squamous cell carcinoma.

compared with the PMR cut-off value for e every candidate gene obtained from the discovery cohort (Fig. 2). Prevalence cohort samples with a ≥PMR value than the PMR cut-off value for every candidate gene were classified as M. Prevalence samples with a lower PMR than the PMR cut-off value for every candidate gene were classified as UM. The prevalence of M candidate genes in HNSCC and normal samples from the prevalence cohort is shown in Table SIV. Promoter aberrant methylation of *DAPK1* was detected in 58.0% of the HNSCC samples (P=0.005), M *CDH1* was detected in 50.0% of the HNSCC samples (P=0.112), methylation of *PAX1* was confirmed in 82.0% of the HNSCC samples (P=0.001), M *CALCA* was confirmed in 44.0% of the HNSCC samples (P=0.036), while M *TIMP3* was confirmed in 76.0% of the HNSCC prevalence cohort samples (P=0.003).

Association analysis between HNSCC clinicopathological characteristics and aberrant methylation of *DAPK1, CDH1, PAX1, CALCA* and *TIMP3* (Table III) shows that the frequency of M *PAX1* was significantly different across HNSCC anatomic subsites (P=0.029), being the highest frequency of detection in LSCC. No significant association was found between aberrant M genes (*DAPK1, CDH1, CALCA* and *TIMP3*) with sex, age, smoking, alcohol abuse, HPV infection and tumor staging. Concurrent methylation of two to five candidate genes was found in 15% of the patients with HNSCC (Fig. S3).

The prognostic value of *DAPK1, CDH1, PAX1, CALCA and TIMP3* was assessed using Kaplan-Meier. Kaplan Meier survival analysis showed that patients with HNSCC and aberrant M *DAPK1* had a better OS (61.0 months) compared with UM *DAPK1* OS (24 months; P=0.043). No significant association with the OS of patients with HNSCC and aberrant methylation of *CDH1, PAX1, CALCA and TIMP3* was found (Fig. 3).

A Cox regression analysis of OS was also performed to evaluate the association between aberrant methylation of the five candidate genes *DAPK1, CDH1, PAX1, CALCA* and *TIMP3*, and the risk of death from HNSCC (Table IV). Clinicopathological indicators such as age, tumor stage and differentiation, smoking, drinking and HPV infection were included in the analysis to assess their effect on HNSCC survival outcomes in this cohort. *DAPK* methylation (P=0.001; HR, 0.096; 95% CI, 0.03-0.37); HPV^- tumors (P=0.006; HR,

Table III. Association between clinicopathological characteristics of the HNSCC cohort (n=50) and aberrant promoter methylation of *DAPK1*, *CDH1*, *PAX1*, *CALCA* and *TIMP3*.

	DAPK1					*CDH1*					*PAX1*					*CALCA*					*TIMP3*				
Clinicopathological characteristics	Meth	Unmeth	Unknown	P-value	RR [95% CI]	Meth	Unmeth	Unknown	P-value	RR [95% CI]	Meth	Unmeth	Unknown	P-value	RR [95% CI]	Meth	Unmeth	Unknown	P-value	RR [95% CI]	Meth	Unmeth	Unknown	P-value	RR [95% CI]
Age, years																									
<60	10	7			1.02	9	8			1.09	15	2			1.12	6	11			0.72	11	6			0.79
≥60	19	14		1.000	[0.62-1.67]	16	17		1.000	[0.62-1.93]	26	7		0.699	[0.87-1.44]	16	17		0.548	[0.35-1.51]	27	6		0.294	[0.54-1.16]
Sex, n																									
Male	27	18			1.50	23	22			1.28	38	7			1.41	19	26			0.70	33	12			0.73
Female	2	3		0.638	[0.50-4.50]	2	3		1.000	[0.42-3.88]	3	2		0.216	[0.68-2.91]	3	2		0.642	[0.32-1.55]	5	0		0.319	[0.61-0.87]
HPV-16 status, n																									
HPV-16^{+}	11	13			0.66	12	12			1.00	19	5			0.93	10	14			0.90	19	5			1.08
HPV-16^{-}	18	8		0.151	[0.39-1.10]	13	13		1.000	[0.57-1.74]	22	4		0.721	[0.72-1.22]	12	14		0.783	[0.48-1.69]	19	7		0.745	[0.79-1.48]
Tumor site, n																									
Oral cavity	8	5				6	7				13	0				4	9				11	2			
Pharynx	3	3				1	5				3	3				4	2				6	0			
Larynx	18	13		0.894		18	13		0.169		25	6		0.029		14	17		0.334		21	10		0.167	
Disease staging, n																									
Early (I/II)	6	5			0.96	6	5			1.12	11	0			1.32	4	7			0.79	10	1			1.29
Late (III/IV)	21	16	2	1.000	[0.52-1.77]	18	19	2	1.000	[0.59-2.11]	28	9	2	0.095	[1.10-1.59]	17	20	2	0.733	[0.34-1.86]	26	11	2	0.248	[0.98-1.71]
Nodal involvement, n																									
Yes	7	3			1.29	5	5			1.02	7	3			0.84	4	6			0.87	6	4			0.77
No	20	17	3	0.481	[0.78-2.14]	18	19	3	1.000	[0.51-2.08]	31	6	3	0.377	[0.54-1.28]	17	20	3	1.000	[0.38-2.01]	29	8	3	0.251	[0.45-1.31]
Tumor differentiation, n																									
Well	6	7				4	9				11	2				3	10				11	2			
Moderate	19	10				17	13				25	5				14	16				22	8			
Poor	2	4	2	0.243		3	3	1	0.296		4	2	1	0.597		4	2	1	0.162		4	2	1	0.633	
Heavy smoking, n																									
Yes	25	18			1.74	23	20			8.02	35	8			1.22	19	24			0.66	32	10			1.14
No	1	2	4	0.572	[0.34-8.82]	0	3	4	0.233	[0.39-164.9]	2	1	4	0.488	[0.54-2.75]	2	1	4	0.585	[0.28-1.58]	2	1	5	1.000	[0.50-2.59]
Heavy drinking, n																									
Yes	22	16			1.16	21	17			2.21	32	6			1.35	16	22			0.67	28	10			0.98
No	4	4	4	0.713	[0.55-2.43]	2	6	4	0.243	[0.64-7.59]	5	3	4	0.176	[0.77-2.35]	5	3	4	0.439	[0.35-1.30]	6	2	4	1.000	[0.63-1.53]

Unknown = patients with HNSCC and no available clinicopathological characteristics. HNSCC, head and neck squamous cell carcinoma; HPV, human papillomavirus; CI, confidence interval; meth, methylated; unmeth, unmethylated; RR, relative risk.

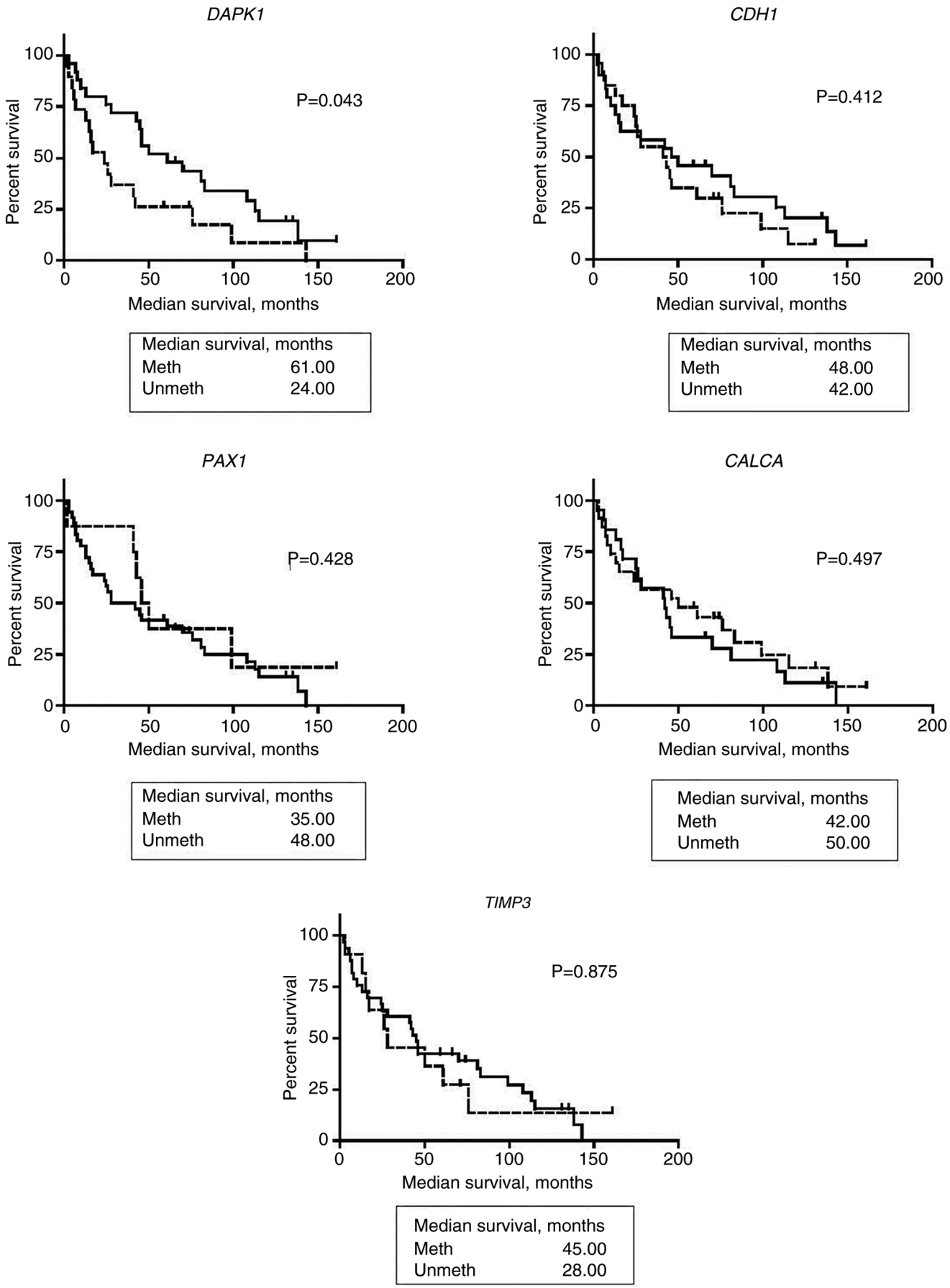

Figure 3. Overall survival of patients with HNSCC according to the aberrant promoter methylation status *of DAPK1*, *CDH1*, *PAX1*, *CALCA*, and *TIMP3*. Kaplan-Meier survival curve analysis of patients with HNSCC and aberrantly meth genes vs. patients with HNSCC and unmeth genes. The black line represents patients with meth HNSCC and the dashed black line represents patients with unmeth HNSCC. Median survival in each curve is represented in months. Meth, methylated; unmeth, unmethylated; HNSCC, head and neck squamous cell carcinoma.

Table IV. Cox regression analysis of overall survival.

Variables	P-value	HR [95% CI]
DAPK1 meth	0.001[a]	0.096 [0.03-0.37]
CDH1 meth	0.110	2.990 [0.78-11.48]
PAX1 meth	0.825	1.230 [0.20-7.55]
TIMP3 meth	0.951	1.040 [0.30-3.66]
CALCA meth	0.259	0.500 [0.15-1.68]
HPV-16$^-$	0.006[a]	9.720 [1.94-48.72]
Tumor site		
Larynx	0.765	1.360 [0.18-9.98]
Oral Cavity	0.920	0.870 [0.06-13.30]
Pharynx	0.033[a]	14.170 [1.25-161.15]
Tumor differentiation		
Well	0.226	2.760 [0.53-14.27]
Moderate	0.013[a]	8.560 [1.58-46.46]
Tumor stage		
I	0.997	1.000 [0.05-19.80]
II	0.324	3.080 [0.03-28.90]
III	0.668	1.500 [0.24-9.37]
Positive lymph nodes	0.401	0.490 [0.09-2.61]
Heavy smoking	0.969	0.940 [0.05-16.71]
Heavy drinking	0.523	1.720 [0.33-9.10]
Age	0.002[a]	1.110 [1.04-1.18]

[a]Indicates a statistically significant difference (P<0.05). Meth, methylated; HPV, human papillomavirus; HR, hazard ratio; CI, confidence interval.

9.72; 95% CI, 1.94-48.42); tumor site (P=0.033; HR, 0.96; 95% CI, 0.03-0.37); tumor differentiation (P=0.013; HR, 8.56; 95% CI, 1.58-46.46); and age (P=0.002; HR, 1.11; 95% CI, 1.04-1.18) showed significant HRs.

Discussion

HNSCC is a heterogeneous disease comprising tumors from multiple anatomic subsites, each differing in prognosis and treatment strategy. Aberrant DNA methylation changes have been shown useful as molecular classifiers in several tumor sites because of their predictive capacity for disease detection, patient prognosis and treatment response (56-58). The discovery of epigenetic alterations is critical for a better understanding of HNSCC initiation and progression. Thus, the identification of genes epigenetically inactivated as potential prognostic biomarkers for HNSCC is urgent.

In the current study, an epigenomic analysis of a well-defined HNSCC cohort was shown. A genome-wide DNA methylation analysis showed that HNSCC tumors have 2,565 DMRs common to all HNSCC subsites. Several critical DMRs associated with a specific HNSCC anatomical subsite were identified. A total of 889, 363 and 738 DMRs unique to OSCC, OPSCC and LSCC were identified, respectively. These DMRs were associated with critical cellular pathways, often deregulated in multiple cancer types, including HNSCC (59). Among those DMRs, 10 candidate genes (*DAPK1, PITX2, PAX5, TIMP3, SFRP1, CALCA, SOCS1, CDH1, MAGI2* and *PAX1)* were selected and evaluated further for their predictive and prognostic value.

Kaplan-Meier survival analysis (P=0.043) and Cox regression analysis of OS (P=0.001) showed that *DAPK1* methylation is associated with better prognosis in HNSCC. *DAPK1,* a mediator of a wide range of cellular processes including growth, apoptosis, autophagy and oxidative stress (60,61), was identified as aberrantly methylated in all HNSCC subsites. *DAPK1* prediction analysis suggested high levels of specificity and sensitivity for HNSCC detection, which was later confirmed in the HNSCC prevalence study (P=0.005). Epigenetic inactivation of *DAPK1* may be a key event in head and neck carcinogenesis (62). Aberrant methylation of *DAPK1* has been confirmed in the cancer of the OSCC (63-65), pharynx (66) and larynx (67). Aberrant methylation of *DAPK1* has been shown to occur in advanced HNSCC (stages III and IV) tumors with positive lymph node involvement, resulting in a poor prognosis (67). Likewise, downregulation of *DAPK1* expression has also been shown in HNSCCs (68,69). Loss of *DAPK1* expression, mediated by promoter hypermethylation, has been associated with deregulation of autophagy in cancer cells and resistance to radiotherapy and chemotherapy treatments (70). Thus, aberrantly methylated *DAPK1* may be associated with HNSCC carcinogenesis and progression.

Preliminary data from our research group suggested that aberrantly M *CDH1* was associated with worse outcome (death) in LSCC. The present study shows that *CDH1* is frequently M in LSCC. *CDH1*, a tumor invasion/suppressor gene, transcribes a 120-kDa glycoprotein, E-cadherin (71), that is essential for establishing and maintaining intercellular connections (72). Squamous carcinoma cells are characterized by poor cellular adhesion, loss of epithelial morphology and increased cellular motility (73). Downregulation of E-cadherin expression, either by genetic mutation or epigenetic dysregulation, leads to alterations in cell-to-cell adhesion and increases the metastatic potential of squamous cell carcinoma. M *CDH1* has been associated with invasive LSCC tumors (Grade 3 and 4) and metastasis (74). M *CDH1* has also been detected in tissue samples of surrounding mucosa of OSCC, suggesting that M *CDH1* may be a key contributor to HNSCC carcinogenesis. Downregulation of *CDH1* expression has been observed in HNSCC, and loss of *CDH1* expression was associated with invasive HNSCC (75). Low *CDH1* mRNA levels were detected in patients with tongue cancer (76), but no statistically significant association with clinicopathological characteristics nor patient outcome were found. A meta-analysis of 23 studies showed that *CDH1* methylation was notably more frequent in HNSCC tissue than healthy controls, thus, supporting the role of *CDH1* as a diagnostic biomarker (77). That meta-analysis showed that Asians display a higher frequency of M*CDH1* than Caucasian or African subgroups and suggested that ethnicity may account for the differences in *CDH1* methylation frequency (77). In the present study, it was confirmed that *CDH1* is methylated at high levels in LSCC tumors and could act as a promising prognostic biomarker of LSCC.

The findings of the current study suggest that M *PAX1* is also a promising biomarker for LSCC. M *PAX1* was mostly detected in LSCC and was significantly different than control

samples (P≤0.001). The frequency of M *PAX1* was significantly different across HNSCC subsites, showing a higher frequency in LSCC (P=0.029) corroborating the genome-wide analysis. The results of the present study show that aberrant methylation of *PAX1* had predictive accuracy for identifying HNSCC samples (ROC, 1.00; 100% specificity and sensitivity). *PAX1* belongs to the highly conserved PAX gene family, which are developmentally controlled and encode transcription factors regulating embryogenesis in vertebrates (78). The expression of *PAX1* during the development process is limited to the skeleton, thymus and parathyroid glands (79). *PAX1*, among other *PAX* genes, has critical roles in the development of the thymus and the parathyroid gland (80). *PAX1* dysregulation causes a hypoplastic thymus with defects in thymocyte maturation and a delay in separation from the oropharynx (81), suggesting that loss of *PAX1* dysregulates proliferation of the thymus (82). Loss of *PAX1* expression, mediated by aberrant promoter methylation, has been detected in multiple cancer types, including cervical, colorectal and esophageal cancer, and in HNSCC (83,84). It has been shown that *PAX1* is aberrantly M in HSCCC, including PAX1 aberrant methylation association with a higher risk of HNSCC (85,86). *PAX1* methylation has been mostly studied in OSCC and associated with larger tumor size (87-89).

PAX1 methylation has been studied in HPV$^+$ cervical cancer in which HPV infection disrupts epigenetic regulation through a series of aberrant methylation changes in the host genome (90). Likewise, HPV-induced aberrant methylation may affect the carcinogenic activity and clinical manifestation of HPV$^+$ HNSCC and distinguish it from HPV$^-$ HNSCC. Currently in Taiwan, M *PAX1* is used for cervical cancer screening due to its association with increasing cervical dysplasia. Likewise, the association of M *PAX1* with HPV infection in cervical cancer suggests that HPV may regulate PAX1 methylation; thus, further analysis of the significance of M *PAX1* in HPV$^+$ patients with HNSCC is warranted.

Among other candidate genes evaluated, *CALCA*, a potent vasodilator, and an essential inflammatory response molecule (91), was predicted as particularly M in OPSCC. Detection of aberrantly M *CALCA* in HNSCC showed to be highly accurate with 100% specificity and 85% sensitivity (P=0.0006). M *CALCA* was detected in 79% of the 19 OPSCC tumor samples, corroborating the predictive analysis. Additional assessment in 50 HNSCC samples showed that M *CALCA* was predominant in 48% of HNSCC samples (P=0.036). M *CALCA* has been detected in leukemia, testicular, bladder, non-small cell lung, thyroid, and head and neck cancer (92-97). In leukemia, M *CALCA* has been associated with disease relapse and poor prognosis (98,99). Likewise, studies in non-small lung carcinoma reveal that M *CALCA* was more common in squamous cell carcinomas than adenocarcinomas (100). Furthermore, M *CALCA* was associated with a poor prognosis in non-small lung carcinoma independent of the tumor stage (101). Aberrant methylation of *CALCA* in HNSCC has been studied mostly in oral cancer samples. Guerrero-Preston *et al* (102) showed a higher frequency of M *CALCA* in OSCC, although the prognostic value for HNSCC was not discussed. An additional study showed that M *CALCA* was associated with metastasis and a poorer prognosis in OSCC (103). Thus, the prognostic value of *CALCA* in HNSCC demands further study, particularly in OPSCC.

M *TIMP3*, a tissue inhibitor of metalloproteinase 3, was significantly detected in HNSCC (76%; P=0.003). The frequency of M *TIMP3* was higher in OSCC (85%) compared with other subsites and corroborated the genome-wide analysis. Previous studies have shown M *TIMP3* in HNSCC (104) in addition to various tumor types, including kidney, brain and esophageal cancer (105,106). *TIMP3* is a critical regulator of inflammation (107,108), and loss of *TIMP3* expression has been associated with an increase in cell proliferation, tumor growth, angiogenesis and metastasis (109-112). No significant association was identified between M *TIMP3* and HNSCC clinical features in the cohort of the present study. Previous studies have detected M *TIMP3* more frequently in tumor tissue of patients with early-stage (I/II) HNSCC compared with healthy saliva samples (113,114) but they did not find a clinical association with cancer. A study characterizing the epigenome in HPV$^+$ patients with HNSCC showed that aberrant *TIMP3* was predominant in HPV$^+$ patients (115). The authors showed that M *TIMP3* was associated with positive lymph node spread, and consequently, with a poorer prognosis. Therefore, further studies of M *TIMP3* in HPV$^+$ and HPV$^-$ patients with HNSCC are warranted.

The current study also assessed the aberrant methylation of *SFRP1, MAGI2, PITX2* and *PAX5* in HNSCC. In OSCC, M *PAX5* was detected in 79.3% of tumor samples, and M *PITX2* was detected in 58.6% of OSCC samples. M *MAGI2* was detected in 64.1% of LSCCs, and aberrant M *SFRP1* was detected in 84.2% of oroOPSCC samples. The predictive accuracy of *SFRP1, MAGI2, PITX2* and *PAX5* was significant, and it should be further explored in a larger HNSCC cohort to assess their predictive value accurately.

Cox regression analysis of OS revealed that HPV$^-$ patients with HNSCC were at a higher risk of dying of cancer (P=0.006; HR, 9.72; 95% CI, 1.94-48.42) compared to HPV$^+$ patients with HNSCC. Previous studies have shown that HPV$^+$ tumors have higher methylation levels due to an overexpression of DNMT3a (116-118). HPV$^+$ tumors commonly inactivate *CDKN2A* by hypermethylation, whereas HPV$^-$ tumors mostly inactivate *CDKN2A* by deletions or mutations (119). Likewise, studies have shown that HPV$^-$ tumors have a global hypomethylation state and higher genomic instability compared with HPV$^+$ tumors (120-122). It has been proposed that the machinery of HPV$^+$ cells re-establish developmental methylation patterns as a defense mechanism to abolish transcription of the virus (122), which results in increased DNA methylation. Differences in DNA methylation patterns between HPV$^+$ and HPV$^-$ HNSCC must be substantiated and analyzed for their potential clinical translation into targeted treatment options.

In summary, the findings of the current study suggest that distinctive aberrant DNA methylation profiles arise within every head and neck cancer anatomic subsite, thus explaining the disease heterogeneity and possible association with disease progression or response to treatment. It was also shown that *DAPK1, CDH1, PAX1, CALCA* and *TIMP3* are frequently aberrantly M in patients with head and neck cancer and influence survival. *PAX1* hypermethylation was different across HNSCC anatomic subsites (P=0.029), and predominantly detected in LSCC. Kaplan-Meier survival analysis (P=0.043)

and Cox regression analysis of OS (P=0.001) showed that *DAPK1* methylation is associated with better prognosis in HNSCC.

The main limitation of the current study was the small sample size. Further studies with larger cohorts are needed to validate the results obtained. Determination of the global epigenetic landscape of HNSCC will require large cohorts of samples and coordinated research efforts to predict better biomarkers for disease outcome and targeted therapeutic interventions. Furthermore, epigenomic studies in which HNSCC tumors are stratified by anatomic site and HPV positivity are needed to better understand the modulation of the host epigenome by HPV modifying, and subsequent impact in disease progression and severity.

Acknowledgements

Not applicable.

Funding

The present study was supported in part by the University of Puerto Rico School of Medicine Department of Surgery Otolaryngology Section; NIH/National Cancer Institute (grant nos. P20CA91402, U54CA96297, K01CA164092, R44CA254690, R44CA281719 and U01CA84986), the NIH/National Institute of General Medical Sciences (grant no. S06GM8224), the NIH/National Institute of Dental and Craniofacial Research Award (grant no. RC2DE20957) and the NIH/National Institute of Minority Health and Disparities (grant no. R44MD014911). Bianca Rivera Peña's research was supported in part by the NIGMS-RISE award (grant no. R25 GM061838). This research used core facilities supported by NIH/NCRR and NIH/NIMHDD awards.

Availability of data and materials

The data that support the findings of this study are available from LifeGeneBiomarks, but restrictions apply to the availability of these data, which were used under license for the current study, and so are not publicly available. Data are however available from the authors upon reasonable request and with permission of LifeGeneBiomarks.

Authors' contributions

BRP, RGP, DS and AB performed the study design. AB and JAAO obtained informed consent from patients with HNSCC and healthy individuals. BRP and AB collected all HNSCC tumor and healthy oral samples. BRP, RV, JAAO and RL carried out DNA extraction from HNSCC and healthy samples. BRP, OF and FP carried out the MeDIP assay, hybridization and scanning of samples to the microarray. BRP, NT and RGP performed bioinformatics analysis. RJRB and MEF analyzed the data. BRP, NT, SRT and RGP performed GO analysis, TCGA and Cancer Genome Browser analysis. DS financially supported this study and revised and approved final manuscript. BRP, DS and RGP confirm the authenticity of all the raw data. All authors read and approved the final manuscript.

Ethics approval and consent to participate

All procedures described in the present study were approved by the University of Puerto Rico-Medical Sciences Campus IRB (approval no. MSC-IRB Protocol 2770103). Written informed consent was obtained from all study participants.

Patient consent for publication

Not applicable.

Competing interests

The authors declare that they have no competing interests.

References

1. Bray F, Ferlay J, Soerjomataram I, Siegel RL, Torre LA and Jemal A: Global cancer statistics 2018: GLOBOCAN estimates of incidence and mortality worldwide for 36 cancers in 185 countries. CA Cancer J Clin 68: 394-424, 2018.
2. O'Rorke MA, Ellison MV, Murray LJ, Moran M, James J and Anderson LA: Human papillomavirus related head and neck cancer survival: A systematic review and meta-analysis. Oral Oncol 48: 1191-1201, 2012.
3. Báez A: Genetic and environmental factors in head and neck cancer genesis. J Environ Sci Health C Environ Carcinog Ecotoxicol Rev 26: 174-200, 2008.
4. Saracci R: The interactions of tobacco smoking and other agents in cancer etiology. Epidemiol Rev 9: 175-193, 1987.
5. Blot WJ, McLaughlin JK, Winn DM, Austin DF, Greenberg RS, Preston-Martin S, Bernstein L, Schoenberg JB, Stemhagen A and Fraumeni JF Jr: Smoking and drinking in relation to oral and pharyngeal cancer. Cancer Res 48: 3282-3287, 1988.
6. Hashibe M, Brennan P, Benhamou S, Castellsague X, Chen C, Curado MP, Dal Maso L, Daudt AW, Fabianova E, Fernandez L, *et al*: Alcohol drinking in never users of tobacco, cigarette smoking in never drinkers, and the risk of head and neck cancer: Pooled analysis in the International Head and Neck Cancer Epidemiology Consortium. J Natl Cancer Inst 99: 777-789, 2007.
7. Gillison ML, Koch WM, Capone RB, Spafford M, Westra WH, Wu L, Zahurak ML, Daniel RW, Viglione M, Symer DE, *et al*: Evidence for a causal association between human papillomavirus and a subset of head and neck cancers. J Natl Cancer Inst 92: 709-720, 2000.
8. Mork J, Lie AK, Glattre E, Hallmans G, Jellum E, Koskela P, Møller B, Pukkala E, Schiller JT, Youngman L, *et al*: Human papillomavirus infection as a risk factor for squamous-cell carcinoma of the head and neck. N Engl J Med 344: 1125-1131, 2001.
9. Báez A, Almodóvar JI, Cantor A, Celestin F, Cruz-Cruz L, Fonseca S, Trinidad-Pinedo J and Vega W: High frequency of HPV16-associated head and neck squamous cell carcinoma in the Puerto Rican population. Head Neck 26: 778-784, 2004.
10. Rivera-Peña B, Ruíz-Fullana FJ, Vélez-Reyes GL, Rodriguez-Benitez RJ, Marcos-Martínez MJ, Trinidad-Pinedo J and Báez A: HPV-16 infection modifies overall survival of Puerto Rican HNSCC patients. Infect Agent Cancer 11: 47, 2004.
11. Siegel RL, Miller KD and Jemal A: Cancer statistics, 2017. CA Cancer J Clin 67: 7-30, 2017.
12. Park A, Alabaster A, Shen H, Mell LK and Katzel JA: Undertreatment of women with locoregionally advanced head and neck cancer. Cancer 125: 3033-3039, 2019.
13. Katzel JA, Merchant M, Chaturvedi AK and Silverberg MJ: Contribution of demographic and behavioral factors on the changing incidence rates of oropharyngeal and oral cavity cancers in northern California. Cancer Epidemiol Biomarkers Prev 24: 978-984, 2015.
14. Dayyani F, Etzel CJ, Liu M, Ho CH, Lippman SM and Tsao AS: Meta-analysis of the impact of human papillomavirus (HPV) on cancer risk and overall survival in head and neck squamous cell carcinomas (HNSCC). Head Neck Oncol 2: 15, 2010.
15. Shiboski CH, Schmidt BL and Jordan RC: Tongue and tonsil carcinoma: Increasing trends in the U.S. population ages 20-44 years. Cancer 103: 1843-1849, 2005.

16. American Joint Committee on Cancer. AJCC Cancer Staging Manual 8. New York, Springer, 2016.
17. Baliga S, Yildiz VO, Bazan J, Palmer JD, Jhawar SR, Konieczkowski DJ, Grecula J, Blakaj DM, Mitchell D, Henson C, *et al*: Disparities in survival outcomes among Racial/Ethnic minorities with head and neck squamous cell cancer in the united states. Cancers (Basel) 15: 1781, 2023.
18. Suárez E, Calo WA, Hernández EY, Diaz EC, Figueroa NR and Ortiz AP: Age-standardized incidence and mortality rates of oral and pharyngeal cancer in Puerto Rico and among Non-Hispanics Whites, Non-Hispanic Blacks, and Hispanics in the USA. BMC Cancer 9: 129, 2009.
19. Fernandez AF, Assenov Y, Martin-Subero JI, Balint B, Siebert R, Taniguchi H, Yamamoto H, Hidalgo M, Tan AC, Galm O, *et al*: A DNA methylation fingerprint of 1628 human samples. Genome Res 22: 407-419, 2012.
20. Taby R and Issa JP: Cancer epigenetics. CA Cancer J Clin 60: 376-392, 2010.
21. Ibáñez de Cáceres I and Cairns P: Methylated DNA sequences for early cancer detection, molecular classification and chemotherapy response prediction. Clin Transl Oncol 9: 429-437, 2007.
22. Calmon MF, Colombo J, Carvalho F, Souza FP, Filho JF, Fukuyama EE, Camargo AA, Caballero OL, Tajara EH, Cordeiro JA and Rahal P: Methylation profile of genes CDKN2A (p14 and p16), DAPK1, CDH1, and ADAM23 in head and neck cancer. Cancer Genet Cytogenet 173: 31-37, 2007.
23. Demokan S and Dalay N: Role of DNA methylation in head and neck cancer. Clin Epigenetics 2: 123-150, 2011.
24. Ovchinnikov DA, Cooper MA, Pandit P, Coman WB, Cooper-White JJ, Keith P, Wolvetang EJ, Slowey PD and Punyadeera C: Tumor-suppressor gene promoter hypermethylation in saliva of head and neck cancer patients. Transl Oncol 5: 321-326, 2012.
25. Herman JG and Baylin SB: Gene silencing in cancer in association with promoter hypermethylation. N Engl J Med 349: 2042-2054, 2003.
26. Esteller M: Epigenetics in cancer. N Engl J Med 358: 1148-1159, 2008.
27. Lleras RA, Smith RV, Adrien LR, Schlecht NF, Burk RD, Harris TM, Childs G, Prystowsky MB and Belbin TJ: Unique DNA methylation loci distinguish anatomic site and HPV status in head and neck squamous cell carcinoma. Clin Cancer Res 19: 5444-5455, 2013.
28. Bernabe RD: INK4a/ARF/INK4b tumor suppressor locus: Its potential role in head and neck cancer tumorigenesis (Doctoral dissertation) (order no. 3221909). ProQuest Dissertations and Theses Global, 2006. Available from https://search.proquest.com/docview/304984294?accountid=44820.
29. Rivera-Peña B and Báez A: Abstract 4793: Aberrant methylation of CDH1 correlates with poor prognosis in patients with head and neck squamous cell carcinoma (abstract). In: Proceedings of the 102nd Annual Meeting of the American Association for Cancer Research. Cancer Res 71 (Suppl 8): 4793-4793, 2011.
30. Irizarry RA, Ladd-Acosta C, Carvalho B, Wu H, Brandenburg SA, Jeddeloh JA, Wen B and Feinberg AP: Comprehensive high-throughput arrays for relative methylation (CHARM). Genome Res 18: 780-790, 2008.
31. Jaffe AE, Murakami P, Lee H, Leek JT, Fallin MD, Feinberg AP and Irizarry RA: Bump hunting to identify differentially methylated regions in epigenetic epidemiology studies. Int J Epidemiol 41: 200-209, 2012.
32. Du P, Zhang X, Huang CC, Jafari N, Kibbe WA, Hou L and Lin SM: Comparison of Beta-value and M-value methods for quantifying methylation levels by microarray analysis. BMC Bioinformatics 11: 587, 2010.
33. The Cancer Genome Atlas Network: Comprehensive genomic characterization of head and neck squamous cell carcinomas. Nature 517: 576-582, 2015.
34. Aryee MJ, Jaffe AE, Corrada-Bravo H, Ladd-Acosta C, Feinberg AP, Hansen KD and Irizarry RA: Minfi: A flexible and comprehensive Bioconductor package for the analysis of Infinium DNA methylation microarrays. Bioinformatics 30: 1363-1369, 2014.
35. Eads CA, Danenberg KD, Kawakami K, Saltz LB, Blake C, Shibata D, Danenberg PV and Laird PW: MethyLight: A high-throughput assay to measure DNA methylation. Nucleic Acids Res 28: E32, 2000.
36. Rettori MM, de Carvalho AC, Longo AL, de Oliveira CZ, Kowalski LP, Carvalho AL and Vettore AL: TIMP3 and CCNA1 hypermethylation in HNSCC is associated with an increased incidence of second primary tumors. J Transl Med 11: 316, 2013.
37. Li LC and Dahiya R: MethPrimer: Designing primers for methylation PCRs. Bioinformatics 18: 1427-1431, 2002.
38. Valle B, Rodriguez-Torres S, Kuhn E, Díaz-Montes T, Parrilla-Castellar E, Lawson F, Folawiyo O, Ili-Gangas C, Brebi-Mieville P, Eshleman J, *et al*: HIST1H2BB and MAGI2 methylation and somatic mutations as precision medicine biomarkers for diagnosis and prognosis of high-grade serous ovarian cancer. Cancer Prev Res (Phila) 13: 783-794, 2020.
39. Guerrero-Preston R, Valle BL, Jedlicka A, Turaga N, Folawiyo O, Pirini F, Lawson F, Vergura A, Noordhuis M, Dziedzic A, *et al*: Molecular triage of premalignant lesions in Liquid-Based cervical cytology and circulating Cell-Free DNA from urine, using a panel of methylated human papilloma virus and host genes. Cancer Prev Res (Phila) 9: 915-924, 2016.
40. Guerrero-Preston R, Michailidi C, Marchionni L, Pickering CR, Frederick MJ, Myers JN, Yegnasubramanian S, Hadar T, Noordhuis MG, Zizkova V, *et al*: Key tumor suppressor genes inactivated by 'greater promoter' methylation and somatic mutations in head and neck cancer. Epigenetics 9: 1031-1046, 2014.
41. Anglim PP, Galler JS, Koss MN, Hagen JA, Turla S, Campan M, Weisenberger DJ, Laird PW, Siegmund KD and Laird-Offringa IA: Identification of a panel of sensitive and specific DNA methylation markers for squamous cell lung cancer. Mol Cancer 7: 62, 2008.
42. Müller HM, Widschwendter A, Fiegl H, Ivarsson L, Goebel G, Perkmann E, Marth C and Widschwendter M: DNA methylation in serum of breast cancer patients: An independent prognostic marker. Cancer Res 63: 7641-7665, 2003.
43. Eads CA, Lord RV, Wickramasinghe K, Long TI, Kurumboor SK, Bernstein L, Peters JH, DeMeester SR, DeMeester TR, Skinner KA and Laird PW: Epigenetic patterns in the progression of esophageal adenocarcinoma. Cancer Res 61: 3410-3418, 2001.
44. van Asperen CJ, Brohet RM, Meijers-Heijboer EJ, Hoogerbrugge N, Verhoef S, Vasen HF, Ausems MG, Menko FH, Gomez Garcia EB, Klijn JG, *et al*: Cancer risks in BRCA2 families: Estimates for sites other than breast and ovary. J Med Genet 42: 711-719, 2005.
45. Seiwert TY, Zuo Z, Keck MK, Khattri A, Pedamallu CS, Stricker T, Brown C, Pugh TJ, Stojanov P, Cho J, *et al*: Integrative and comparative genomic analysis of HPV-positive and HPV-negative head and neck squamous cell carcinomas. Clin Cancer Res 21: 632-641, 2015.
46. Califano J, Van Der Riet P, Westra W, Nawroz H, Clayman G, Piantadosi S, Corio R, Lee D, Greenberg B, Koch W and Sidransky D: Genetic progression model for head and neck cancer: Implications for field cancerization. Cancer Res 56: 2488-2492, 1996.
47. Cai F, Xiao X, Niu X and Zhong Y: Association between promoter methylation of DAPK gene and HNSCC: A meta-analysis. PLoS One 12: e0173194, 2017.
48. Ngan HL, Liu Y, Fong AY, Poon PHY, Yeung CK, Chan SSM, Lau A, Piao W, Li H, Tse J, *et al*: MAPK pathway mutations in head and neck cancer affect immune microenvironments and ErbB3 signaling. Life Sci Alliance 3: e201900545, 2020.
49. Cilona M, Locatello LG, Novelli L and Gallo O: The mismatch repair system (MMR) in head and neck carcinogenesis and its role in modulating the response to immunotherapy: A critical review. Cancers (Basel) 12: 3006, 2020.
50. Meng RW, Li YC, Chen X, Huang YX, Shi H, Du DD, Niu X, Lu C and Lu MX: Aberrant Methylation of RASSF1A closely associated with HNSCC, a Meta-Analysis. Sci Rep 6: 20756, 2016.
51. Moon SM, Kim SA, Yoon JH and Ahn SG: HOXC6 is deregulated in human head and neck squamous cell carcinoma and modulates Bcl-2 expression. J Biol Chem 287: 35678-35688, 2012.
52. Carla C, Daris F, Cecilia B, Francesca B, Francesca C and Paolo F: Angiogenesis in head and neck cancer: A review of the literature. J Oncol 2012: 358472, 2012.
53. Mineta H, Miura K, Ogino T, Takebayashi S, Misawa K, Ueda Y, Suzuki I, Dictor M, Borg A and Wennerberg J: Prognostic value of vascular endothelial growth factor (VEGF) in head and neck squamous cell carcinomas. Br J Cancer 83: 775-781, 2000.
54. Iwai S, Katagiri W, Kong C, Amekawa S, Nakazawa M and Yura Y: Mutations of the APC, beta-catenin, and axin 1 genes and cytoplasmic accumulation of beta-catenin in oral squamous cell carcinoma. J Cancer Res Clin Oncol 131: 773-782, 2005.
55. Leethanakul C, Patel V, Gillespie J, Pallente M, Ensley JF, Koontongkaew S, Liotta LA, Emmert-Buck M and Gutkind JS: Distinct pattern of expression of differentiation and growthrelated genes in squamous cell carcinomas of the head and neck revealed by the use of laser capture microdissection and cDNA arrays. Oncogene 19: 3220-3224, 2000.

56. Paska AV and Hudler P: Aberrant methylation patterns in cancer: A clinical view. Biochem Med (Zagreb) 25: 161-176, 2015.
57. Hao X, Luo H, Krawczyk M, Wei W, Wang W, Wang J, Flagg K, Hou J, Zhang H, Yi S, *et al*: DNA methylation markers for diagnosis and prognosis of common cancers. Proc Natl Acad Sci USA 114: 7414-7419, 2017.
58. Chen D, Wang M, Guo Y, Wu W, Ji X, Dou X, Tang H, Zong Z, Zhang X and Xiong D: An aberrant DNA methylation signature for predicting the prognosis of head and neck squamous cell carcinoma. Cancer Med 10: 5936-5947, 2021.
59. Stadler ME, Patel MR, Couch ME and Hayes DN: Molecular biology of head and neck cancer: Risks and pathways. Hematol Oncol Clin North Am 22: 1099-1124, 2008.
60. Bialik S and Kimchi A: The death-associated protein kinases: Structure, function, and beyond. Annu Rev Biochem 75: 189-210, 2006.
61. Gade P, Manjegowda SB, Nallar SC, Maachani UB, Cross AS and Kalvakolanu DV: Regulation of the death-associated protein kinase 1 expression and autophagy via ATF6 requires apoptosis signal-regulating kinase 1. Mol Cell Biol 34: 4033-448, 2014.
62. Li C, Wang L, Su J, Zhang R, Fu L and Zhou Y: mRNA expression and hypermethylation of tumor suppressor genes apoptosis protease activating factor-1 and death-associated protein kinase in oral squamous cell carcinoma. Oncol Lett 6: 280-286, 2013.
63. Jayaprakash C, Varghese VK, Bellampalli R, Radhakrishnan R, Ray S, Kabekkodu SP and Satyamoorthy K: Hypermethylation of Death-associated protein kinase (DAPK1) and its association with oral carcinogenesis-An experimental and meta-analysis study. Arch Oral Biol 80: 117-129, 2017.
64. Melchers LJ, Clausen MJ, Mastik MF, Slagter-Menkema L, van der Wal JE, Wisman GB, Roodenburg JL and Schuuring E: Identification of methylation markers for the prediction of nodal metastasis in oral and oropharyngeal squamous cell carcinoma. Epigenetics 10: 850-860, 2015.
65. Wei DM, Liu DY, Lei DP, Jin T, Wang J and Pan XL: Aberrant methylation and expression of DAPk1 in human hypopharyngeal squamous cell carcinoma. Acta Otolaryngol 135: 70-78, 2015.
66. van Kempen PM, van Bockel L, Braunius WW, Moelans CB, van Olst M, de Jong R, Stegeman I, van Diest PJ, Grolman W and Willems SM: HPV-positive oropharyngeal squamous cell carcinoma is associated with TIMP3 and CADM1 promoter hypermethylation. Cancer Med 3: 1185-1196, 2014.
67. Stephen JK, Chen KM, Shah V, Havard S, Kapke A, Lu M, Benninger MS and Worsham MJ: DNA hypermethylation markers of poor outcome in laryngeal cancer. Clin Epigenetics 1: 61-69, 2010.
68. Strzelczyk JK, Krakowczyk Ł and Owczarek AJ: Aberrant DNA methylation of the p16, APC, MGMT, TIMP3 and CDH1 gene promoters in tumours and the surgical margins of patients with oral cavity cancer. J Cancer 9: 1896-1904, 2018.
69. Schmezer P and Plass C: Epigenetic aspects in carcinomas of the head and neck. HNO 56: 594-602, 2008 (In German).
70. Singh P, Ravanan P and Talwar P: Death associated protein kinase 1 (DAPK1): A regulator of apoptosis and autophagy. Front Mol Neurosci 9: 46, 2016.
71. Humphries MJ and Newham P: The structure of cell-adhesion molecules. Trends Cell Biol 8: 78-83, 1998.
72. Riethmacher D, Brinkmann V and Birchmeier C: A targeted mutation in the mouse E-cadherin gene results in defective preimplantation development. Proc Natl Acad Sci USA 92: 855-859, 1995.
73. Pećina-Slaus N: Tumor suppressor gene E-cadherin and its role in normal and malignant cells. Cancer Cell Int 3: 17, 2003.
74. Starska K, Forma E, Lewy-Trenda I, Papież P, Woś J and Bryś M: Diagnostic impact of promoter methylation and E-cadherin gene and protein expression levels in laryngeal carcinoma. Contemp Oncol (Pozn) 17: 263-271, 2013.
75. Fan CC, Wang TY, Cheng YA, Jiang SS, Cheng CW, Lee AY and Kao TY: Expression of E-cadherin, Twist, and p53 and their prognostic value in patients with oral squamous cell carcinoma. J Cancer Res Clin Oncol 139: 1735-1744, 2013.
76. Fujii R, Imanishi Y, Shibata K, Sakai N, Sakamoto K, Shigetomi S, Habu N, Otsuka K, Sato Y, Watanabe Y, *et al*: Restoration of E-cadherin expression by selective Cox-2 inhibition and the clinical relevance of the epithelial-to-mesenchymal transition in head and neck squamous cell carcinoma. J Exp Clin Cancer Res 33: 40, 2014.
77. Shen Z, Zhou C, Li J, Deng H, Li Q and Wang J: The association, clinicopathological significance, and diagnostic value of CDH1 promoter methylation in head and neck squamous cell carcinoma: A meta-analysis of 23 studies. Onco Targets Ther 9: 6763-6773, 2016.
78. McGaughran JM, Oates A, Donnai D, Read AP and Tassabehji M: Mutations in PAX1 may be associated with Klippel-Feil syndrome. Eur J Hum Genet 11: 468-474, 2003.
79. Wallin J, Eibel H, Neubüser A, Wilting J, Koseki H and Balling R: Pax1 is expressed during development of the thymus epithelium and is required for normal T-cell maturation. Development 122: 23-30, 1996.
80. Xu J, Xu L, Yang B, Wang L, Lin X and Tu H: Assessing methylation status of PAX1 in cervical scrapings, as a novel diagnostic and predictive biomarker, was closely related to screen cervical cancer. Int J Clin Exp Pathol 8: 1674-1681, 2015.
81. Dietrich S and Gruss P: Undulated phenotypes suggest a role of Pax-1 for the development of vertebral and extravertebral structures. Dev Biol 167: 529-548, 1995.
82. Su D, Ellis S, Napier A, Lee K and Manley NR: Hoxa3 and pax1 regulate epithelial cell death and proliferation during thymus and parathyroid organogenesis. Dev Biol 236: 316-329, 2001.
83. Lorincz AT: Virtues and Weaknesses of DNA methylation as a test for cervical cancer prevention. Acta Cytol 60: 501-512, 2016.
84. Juodzbalys G, Kasradze D, Cicciù M, Šudeikis A, Banys L, Galindo-Moreno P and Guobis Z: Modern molecular biomarkers of head and neck cancer. Part I. Epigenetic diagnostics and prognostics: Systematic review. Cancer Biomark 17: 487-502, 2016.
85. Huang YK, Peng BY, Wu CY, Su CT, Wang HC and Lai HC: DNA methylation of PAX1 as a biomarker for oral squamous cell carcinoma. Clin Oral Investig 18: 801-808, 2014.
86. Sun R, Juan YC, Su YF, Zhang WB, Yu Y, Yang HY, Yu GY and Peng X: Hypermethylated PAX1 and ZNF582 genes in the tissue sample are associated with aggressive progression of oral squamous cell carcinoma. J Oral Pathol Med 49: 751-760, 2020.
87. Cheng SJ, Chang CF, Ko HH, Lee JJ, Chen HM, Wang HJ, Lin HS and Chiang CP: Hypermethylated ZNF582 and PAX1 genes in mouth rinse samples as biomarkers for oral dysplasia and oral cancer detection. Head Neck 40: 355-368, 2018.
88. Morandi L, Gissi D, Tarsitano A, Asioli S, Gabusi A, Marchetti C, Montebugnoli L and Foschini MP: CpG location and methylation level are crucial factors for the early detection of oral squamous cell carcinoma in brushing samples using bisulfite sequencing of a 13-gene panel. Clin Epigenetics 9: 85, 2017.
89. Cheng SJ, Chang CF, Ko HH, Liu YC, Peng HH, Wang HJ, Lin HS and Chiang CP: Hypermethylated ZNF582 and PAX1 genes in oral scrapings collected from cancer-adjacent normal oral mucosal sites are associated with aggressive progression and poor prognosis of oral cancer. Oral Oncol 75: 169-177, 2017.
90. Hsu YW, Huang RL, Su PH, Chen YC, Wang HC, Liao CC and Lai HC: Genotype-specific methylation of HPV in cervical intraepithelial neoplasia. J Gynecol Oncol 28: e56, 2017.
91. Brain SD, Williams TJ, Tippins JR, Morris HR and MacIntyre I: Calcitonin gene-related peptide is a potent vasodilator. Nature 313: 54-56, 1985.
92. Vidal DO, Paixão VA, Brait M, Souto EX, Caballero OL, Lopes LF and Vettore AL: Aberrant methylation in pediatric myelodysplastic syndrome. Leuk Res 31: 175-181, 2007.
93. Martinelli CMDS, Lengert AVH, Cárcano FM, Silva ECA, Brait M, Lopes LF and Vidal DO: MGMT and CALCA promoter methylation are associated with poor prognosis in testicular germ cell tumor patients. Oncotarget 8: 50608-50617, 2016.
94. Brait M, Begum S, Carvalho AL, Dasgupta S, Vettore AL, Czerniak B, Caballero OL, Westra WH, Sidransky D and Hoque MO: Aberrant promoter methylation of multiple genes during pathogenesis of bladder cancer. Cancer Epidemiol Biomarkers Prev 17: 2786-2794, 2008.
95. Wang Y, Zhang D, Zheng W, Luo J, Bai Y and Lu Z: Multiple gene methylation of nonsmall cell lung cancers evaluated with 3-dimensional microarray. Cancer 112: 1325-1336, 2008.
96. Zhang B, Liu S, Zhang Z, Wei J, Qu Y, Wu K, Yang Q, Hou P and Shi B: Analysis of BRAF(V600E) mutation and DNA methylation improves the diagnostics of thyroid fine needle aspiration biopsies. Diagn Pathol 9: 45, 2014.
97. Loyo M, Brait M, Kim MS, Ostrow KL, Jie CC, Chuang AY, Califano JA, Liégeois NJ, Begum S, Westra WH, *et al*: Asurvey of methylated candidate tumor suppressor genes in nasopharyngeal carcinoma. Int J Cancer 128: 1393-1403, 2011.
98. Ismail EA, El-Mogy MI, Mohamed DS and El-Farrash RA: Methylation pattern of calcitonin (CALCA) gene in pediatric acute leukemia. J Pediatr Hematol Oncol 33: 534-542, 2011.
99. Paixão VA, Vidal DO, Caballero OL, Vettore AL, Tone LG, Ribeiro KB and Lopes LF: Hypermethylation of CpG island in the promoter region of CALCA in acute lymphoblastic leukemia with central nervous system (CNS) infiltration correlates with poorer prognosis. Leuk Res 30: 891-894, 2006.

100. Ji M, Guan H, Gao C, Shi B and Hou P: Highly frequent promoter methylation and PIK3CA amplification in non-small cell lung cancer (NSCLC). BMC Cancer 11: 147, 2011.
101. Morán A, Fernández-Marcelo T, Carro J, De Juan C, Pascua I, Head J, Gómez A, Hernando F, Torres AJ, Benito M and Iniesta P: Methylation profiling in non-small cell lung cancer: Clinical implications. Int J Oncol 40: 739-746, 2012.
102. Guerrero-Preston R, Soudry E, Acero J, Orera M, Moreno-López L, Macía-Colón G, Jaffe A, Berdasco M, Ili-Gangas C, Brebi-Mieville P, *et al*: NID2 and HOXA9 promoter hypermethylation as biomarkers for prevention and early detection in oral cavity squamous cell carcinoma tissues and saliva. Cancer Prev Res (Phila) 4: 1061-1072, 2011.
103. Jithesh PV, Risk JM, Schache AG, Dhanda J, Lane B, Liloglou T and Shaw RJ: The epigenetic landscape of oral squamous cell carcinoma. Br J Cancer 108: 370-379, 2013.
104. Esteller M, Corn PG, Baylin SB and Herman JG: A gene hypermethylation profile of human cancer. Cancer Res 61: 3225-3229, 2001.
105. Bachman KE, Herman JG, Corn PG, Merlo A, Costello JF, Cavenee WK, Baylin SB and Graff JR: Methylation-associated silencing of the tissue inhibitor of metalloproteinase-3 gene suggest a suppressor role in kidney, brain, and other human cancers. Cancer Res 59: 798-802, 1999.
106. Darnton SJ, Hardie LJ, Muc RS, Wild CP and Casson AG: Tissue inhibitor of metalloproteinase-3 (TIMP-3) gene is methylated in the development of esophageal adenocarcinoma: Loss of expression correlates with poor prognosis. Int J Cancer 115: 351-358, 2005.
107. Smookler DS, Mohammed FF, Kassiri Z, Duncan GS, Mak TW and Khokha R: Tissue inhibitor of metalloproteinase 3 regulates TNF-dependent systemic inflammation. J Immunol 176: 721-725, 2006.
108. Mohammed FF, Smookler DS, Taylor SE, Fingleton B, Kassiri Z, Sanchez OH, English JL, Matrisian LM, Au B, Yeh WC and Khokha R: Abnormal TNF activity in Timp3-/-mice leads to chronic hepatic inflammation and failure of liver regeneration. Nat Genet 36: 969-977, 2004.
109. Zhang L, Zhao L, Zhao D, Lin G, Guo B, Li Y, Liang Z, Zhao XJ and Fang X: Inhibition of tumor growth and induction of apoptosis in prostate cancer cell lines by overexpression of tissue inhibitor of matrix metalloproteinase-3. Cancer Gene Ther 17: 171-179, 2010.
110. Ahonen M, Ala-Aho R, Baker AH, George SJ, Grénman R, Saarialho-Kere U and Kähäri VM: Antitumor activity and bystander effect of adenovirally delivered tissue inhibitor of metalloproteinases-3. Mol Ther 5: 705-715, 2002.
111. Spurbeck WW, Ng CY, Strom TS, Vanin EF and Davidoff AM: Enforced expression of tissue inhibitor of matrix metalloproteinase-3 affects functional capillary morphogenesis and inhibits tumor growth in a murine tumor model. Blood 100: 3361-3368, 2002.
112. Bian J, Wang Y, Smith MR, Kim H, Jacobs C, Jackman J, Kung HF, Colburn NH and Sun Y: Suppression of in vivo tumor growth and induction of suspension cell death by tissue inhibitor of metalloproteinases (TIMP)-3. Carcinogenesis 17: 1805-1811, 1996.
113. Arantes LM, de Carvalho AC, Melendez ME, Centrone CC, Góis-Filho JF, Toporcov TN, Caly DN, Tajara EH, Goloni-Bertollo EM and Carvalho AL; GENCAPO: Validation of methylation markers for diagnosis of oral cavity cancer. Eur J Cancer 51: 632-641, 2015.
114. Righini CA, de Fraipont F, Timsit JF, Faure C, Brambilla E, Reyt E and Favrot MC: Tumor-specific methylation in saliva: A promising biomarker for early detection of head and neck cancer recurrence. Clin Cancer Res 13: 1179-1185, 2007.
115. Zhang HZ, Shan CG, Huang AP and Wang JM: Characterization of gene methylation in human papillomavirus associated-head and neck squamous cell carcinoma. Genet Mol Res: 15, 2016 doi: 10.4238/gmr.15038206.
116. Sartor MA, Dolinoy DC, Jones TR, Colacino JA, Prince ME, Carey TE and Rozek LS: Genome-wide methylation and expression differences in HPV(+) and HPV(-) squamous cell carcinoma cell lines are consistent with divergent mechanisms of carcinogenesis. Epigenetics 6: 777-787, 2011.
117. Nakagawa T, Matsusaka K, Misawa K, Ota S, Takane K, Fukuyo M, Rahmutulla B, Shinohara KI, Kunii N, Sakurai D, *et al*: Frequent promoter hypermethylation associated with human papillomavirus infection in pharyngeal cancer. Cancer Lett 407: 21-31, 2017.
118. Nakagawa T, Kurokawa T, Mima M, Imamoto S, Mizokami H, Kondo S, Okamoto Y, Misawa K, Hanazawa T and Kaneda A: DNA Methylation and HPV-Associated Head and Neck Cancer. Microorganisms 9: 801, 2021.
119. Nakahara Y, Shintani S, Mihara M, Ueyama Y and Matsumura T: High frequency of homozygous deletion and methylation of p16(INK4A) gene in oral squamous cell carcinomas. Cancer Lett 163: 221-228, 2001.
120. Richards KL, Zhang B, Baggerly KA, Colella S, Lang JC, Schuller DE and Krahe R: Genome-wide hypomethylation in head and neck cancer is more pronounced in HPV-negative tumors and is associated with genomic instability. PLoS One 4: e4941, 2009.
121. van Kempen PM, Noorlag R, Braunius WW, Stegeman I, Willems SM and Grolman W: Differences in methylation profiles between HPV-positive and HPV-negative oropharynx squamous cell carcinoma: A systematic review. Epigenetics 9: 194-203, 2014.
122. Camuzi D, Buexm LA, Lourenço SQC, Esposti DD, Cuenin C, Lopes MdSA, Manara F, Talukdar FR, Herceg Z, Ribeiro Pinto LF, *et al*: HPV infection leaves a DNA methylation signature in oropharyngeal cancer affecting both coding genes and transposable elements. Cancers 13: 3621, 2021.